Global Stokes Drift and Climate Wave Modeling

Adrean Webb
Dept. of Applied Math, CIRES
adrean.webb@colorado.edu

Baylor Fox-Kemper
Dept. of Atm. and Oceanic Sciences, CIRES
bfk@colorado.edu

I. Introduction

The Stokes drift velocity - the Lagrangian-average fluid velocity induced from wave action - is an important vector component that appears often in wave-averaged dynamics, such as Langmuir turbulence. However, accuracy and data coverage remain challenges in estimating Stokes drift globally and recent research (Hanley et al., 2010, Webb & Fox-Kemper, 2011) has shown that using atmospheric data and the assumption of wave equilibration is not trustworthy, as often the wave state is dominated by developing or remotely-generated swell conditions.

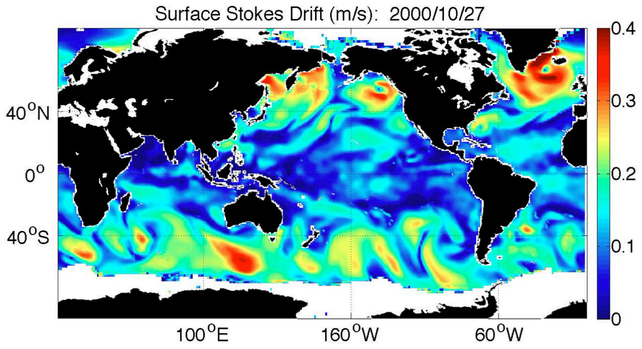

Figure 1: Example of the global variability of Stokes drift (created using WWATCH III and CORE2 winds).

II. Importance for Climate Research

Stokes drift is of interest in climate research due to its dominant role in determining the strength of Langmuir turbulence - surface mixing due to the interaction of wind and waves. Preliminary work (Fox-Kemper et al, 2011) to include this unresolved turbulence in climate models, has shown the potential to correct a well-known, shallow mixed-layer bias in the Southern Ocean.

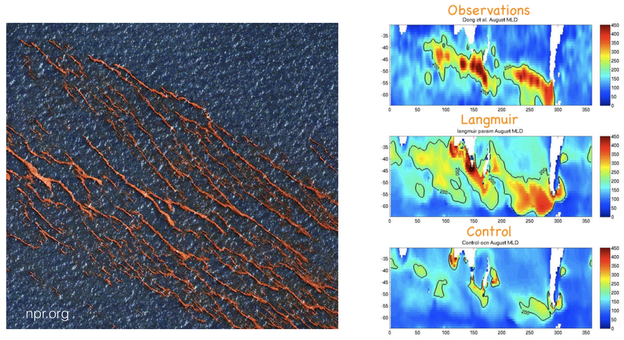

Figure 2: (a) Example of Langmuir turbulence (Deep Water Horizon spill), (b) Southern Ocean mixed-layer depth results from a preliminary parametrization of Langmuir turbulence (NCAR CCSM 3.5)

III. Leading-order Stokes Drift

The Stokes drift can be defined as the mean temporal and spatial difference between the Eulerian and Lagrangian velocities for a finite period and length scale. Using a series expansion and a linear wave decomposition, the leading-order Stokes drift can be rewritten in spectral density form as

$$\boldsymbol{u}^S \approx \frac{16\pi^3}{\mathrm{g}} \int_0^\infty \int_{-\pi}^{\pi} \Big(\cos\theta, \sin\theta, 0\Big) f^3 \, S_{f\theta}(f,\theta) \, e^{\frac{8\pi^2 f^2}{\mathrm{g}} z} d\theta \, df$$

Notice that the leading order Stokes drift is a vector quantity whose magnitude depends both on the directional components of the wave field and the directional spread of wave energy for each component.

To illustrate how different directional wave components might affect the magnitude of Stokes drift, consider a pair of monochromatic waves traveling with an incident angle θ' from the y-axis (Fig. 3). Then the magnitude of Stokes drift will depend on $\sin\theta$'.

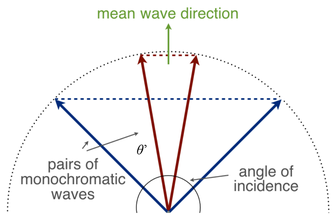

Figure 3: An example of how the directional components of a wave field can affect the magnitude of the Stokes drift.

IV. One-dimensional Stokes Drift

Often only 1D spectral data, or even just spectral moments, are available and this poses a challenge to accurately estimate Stokes drift (see Fig. 4 for example).

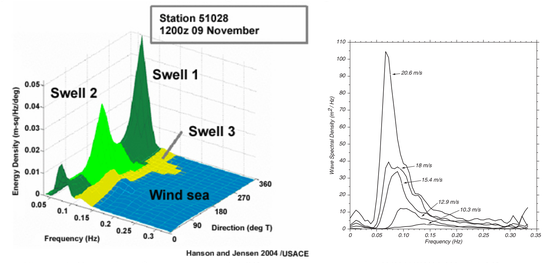

Figure 4: Examples of wave spectra: (a) 2D spectra generated by WWATCH III, (b) 1D Pierson and Moskowitz observational spectra (Stewart, Intro. to Physical Oceanography).

As illustrated previously, 1D estimates will tend to overestimate the full leading-order Stokes drift when there is more than one directional component. However, the error due to wave spreading can be minimized by using an empirical spreading function. Consider splitting the 2D spectral density as

$$\int_0^\infty \int_{-\pi}^{\pi} S_{f\theta}(f,\theta)\, d\theta df \;=\; \int_0^\infty \int_{-\pi}^{\pi} \phi_f(f,\theta)\, S_f(f)\, d\theta df \;=\; \int_0^\infty S_f(f)\, df,$$

where φ_f is the 'directional distribution'. Then a directional loss $\mathbf{H}$ due to wave energy being directed along other directions other than the dominant direction, can be defined as

$$\mathbf{H}(f) = \int_{-\pi}^{\pi} \Big(\cos\theta, \sin\theta, 0\Big) \phi_f(f,\theta)\, d\theta$$

and the 1D Stokes drift approximation can be written as

$$\boldsymbol{u}^s \approx \frac{16\pi^3}{\mathrm{g}} \int_0^\infty \mathbf{H}(f)\, f^3\, S_f(f)\, e^{\frac{8\pi^2 f^2}{\mathrm{g}} z}\, df$$

Commonly, a unidirectional wave approximation ($|\mathbf{H}|$=1) is used to simplify the 1D Stokes drift. However, this tends to overestimate the full leading-order Stokes drift by 33% (in a 3rd generation wave model) and is not recommended (Webb & Fox-Kemper, 2011).

A better approximation can be found by using an empirically-determined frequency-dependent spread function for φ_f. To illustrate, a 'directional loss' is plotted in Fig. 5 using a spread function derived by Donelan et al. (1985).

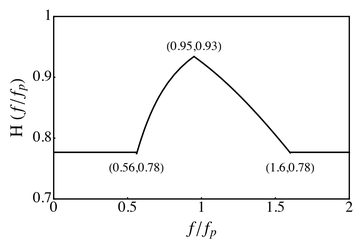

Figure 5: An example of directional spread loss using an empirically-determined spread function from Donelan et al. (1985).

V. Coupling Wave and Circulation Models

For climate research purposes, it is advantageous to use a prognostic 2D wave field - not only to calculate Langmuir turbulence but also to improve atmospheric and oceanic fluxes. As such, NCAR is currently adding a modified form of WWATCH III (v3.14) to the development code of the Community Earth System Model (CESM). The wave module component will be linked to the atmosphere-ocean coupler on 30 minute intervals. Since it is not uncommon for climate runs to span several hundred years, a high model throughput of 30 or more simulated years per computational day is ideal and early benchmarking shows that this is achievable if a coarsened grid of 3.2 x 4 deg is used with a northern and southern latitude cutoff of 70 deg.

30 simulated years per day or greater is necessary to couple with ECSM

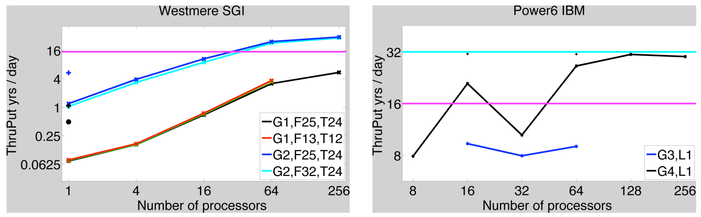

(Lat-lon grids) G1: 1 × 1.25, G2: 1.9 × 2.5, G3: 2.4 × 3, and G4: 3.2 × 4

Figure 6: WWATCH III grid performance with early benchmarking targets on two different machines: (a) NASA Pleaides, (b) NCAR Bluefire. Performance is measured in number of simulated years per day of running.

VI. Need for a Climate Wave Model

Unfortunately, all conventional, structured latitude-longitude-grid wave-models have a disadvantage in that they are singular at the poles and the grid cell sizes shrink appreciably with higher latitudes. This is a problem for climate simulations since the Arctic may be ice-free in the near future and performance of the model will deteriorate as the northern boundary is moved higher. Overcoming these problems and improving performance for long model runs (without compromising climate-scale statistics), remains a challenge.

VII. Unstructured Node Prototype

The previously mentioned disadvantages (pole singularity and shrinking grid cells) are an artifact of representing 3D spherical data on a 2D plane and a decreasing time step due to the CFL condition. One possibility being explored is the use of unstructured nodes on a 3D sphere (both spatial and wavenumber) to remove the singularity and spread the computational costs equally.

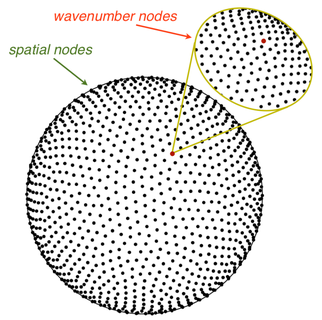

Figure 7: Example of an unstructured node layout to solve the wave action balance equation on an aquaplanet.

Radial basis functions (RBFs) use an arbitrary node layout and are well-suited to solving convective PDEs on a sphere due to their algorithmic simplicity and spectral accuracy. However, the method is computationally expensive when scaled to a large number of 'N' nodes. To circumvent this, the RBF generated finite-difference (RBF-FD) method uses large stencils to generate differential weights to reproduce RBFs (rather than polynomials). This method scales as O(N) per time step and is parallelizable.

Gaussian RBFs are used to define an interpolated solution (in this case, wave spectral density) as

$$\mathcal{N}(\boldsymbol{\alpha}, t)\big|_{t=t_0} = \sum_{i=1}^{N} \lambda_i \, \phi(\|\boldsymbol{\alpha} - \boldsymbol{\alpha}_i\|), \qquad \text{for } \phi(r) = e^{-(\varepsilon r)^2} \text{ and } \varepsilon, r \in \mathbb{R}_+,$$

where $\boldsymbol{\alpha} = (x, y, z, k_x, k_y, k_z)$, ε is the RBF shape parameter, and 'N' is the total number of nodes. The wave action balance equation is then projected on sphere as

$$\partial_t \mathcal{N} + \mathbf{P}\nabla_{\boldsymbol{k}}\,\Omega \cdot \mathbf{P}\nabla_{\boldsymbol{x}}\,\mathcal{N} + \mathbf{P}\nabla_{\boldsymbol{x}}\,\Omega \cdot \mathbf{P}\nabla_{\boldsymbol{k}}\,\mathcal{N} \;=\; \mathbf{P}(\text{Source Terms})$$

and a unique n x n stencil ($n \ll N$) is constructed for each node. For deep water and without currents or source terms, the numerical scheme (with hyperviscosity) becomes

$$\partial_t \underline{\mathcal{N}} = -\underline{c_{g_x}} \circ D_N^x \underline{\mathcal{N}} - \underline{c_{g_y}} \circ D_N^y \underline{\mathcal{N}} - \underline{c_{g_z}} \circ D_N^z \underline{\mathcal{N}}$$

where $\boldsymbol{c_g}$ is the group velocity, '$\circ$' represents element multiplication, and D_N is a sparse N x N differentiation matrix. This can be solved using a parallelized explicit time-stepping method.

VIII. Conclusion

In computations where the accuracy of Stokes drift is important, it is essential to use either the full 2D wave spectra or 1D spectra with an empirically-derived spreading function. Currently, WWATCH III is being coupled to the NCAR CESM to add Langmuir turbulence and improve air-sea fluxes. In addition, a prototype climate wave model is being developed for long model runs and ice-free conditions in the Arctic. While there are still major challenges to overcome (such as boundaries and parallelization), this unstructured node approach shows promise.

Acknowledgements

Thanks to Natasha Flyer at NCAR for advice on implementing the RBF-FD method. Work supported by NASA NNX09AF38G, NSF 0934737, CIRES, UCAR, and CU-Boulder.

References

Fornberg, B., Lehto, E., 2011. Stabilization of RBF-generated finite difference methods for convective PDEs, Journal of Computational Physics, Volume 230, Issue 6.

Donelan, M.A., Hamilton, J., Hui, W.H., 1985. Directional spectra of wind-generated waves. Philosophical Transactions of the Royal Society of London Series A - Mathematical Physical and Enineering Sciences 315, 509-562.

Fox-Kemper, B., Webb, A., Baldwin-Stevens, E., Danabasoglu, G., Hamlington, B., Large, WG., Peacock, S., in preparation. Global climate model sensitivity to estimated Langmuir Mixing. Ocean Modelling.

Hanley, K.E., Belcher, S.E., Sullivan, P.P., 2010. A global climatology of wind–wave interaction. Journal of Physical Oceanography 40, 1263–1282.

Flyer, N., Wright, G., 2009. A Radial Basis Function Method for the Shallow Water Equations on a Sphere. Proceedings of the Royal Society A - Mathematical Physical and Engineering Sciences.

Webb, A., Fox-Kemper, B., 2011. Wave spectral moments and Stokes drift estimation. Ocean Modelling.